Draft version September 1, 2022
Typeset using LATEX **twocolumn** style in AASTeX631

Radio-Loud Active Galactic Nuclei Activity in Merging and Non-Merging Galaxy Cluster

Mary Rickel [1], Emily Moravec [2], Lawrence Bilton,[3] Yjan Gordon,[4] and Martin Hardcastle[5]

[1] *The Ohio State University*
[2] *Green Bank Observatory*
[3] *Pontificia Universidad Católica de Valparaíso*
[4] *University of Wisconsin Madison*
[5] *University of Hertfordshire*

(Received September 1st, 2022)

ABSTRACT

Active Galactic Nuclei (AGN) are by-products of matter accretion onto the central supermassive black hole (SMBH) in a galaxy. AGN fueling is dependent on a variety of factors including the environment of its host galaxy Noordeh et al. (2020). AGN activity is ubiquitously heightened when the host galaxy is a member of a cluster as it provides more opportunities for galaxy-galaxy interactions, as seen in Bilton et al. (2020). This paper examines optically defined AGN sources from Bilton et al. (2020) across 10 low-z galaxy clusters in varying dynamical states to detect and classify Radio Loud AGNs (RLAGNs) using data from the Low Frequency Array (LOFAR) Two-Metre Sky Survey (LoTSS) at 150 MHz. In non-merging galaxy clusters, we find heightened AGN and RLAGN activity.

Keywords: Active Galactic Nuclei – Galaxy Clusters – Radio astronomy

1. INTRODUCTION

1.1. *Active Galactic Nuclei*

It is now well-established that each galaxy hosts a supermassive black hole (SMBH) at its center. In some galaxies, dense matter is accreted onto the central rotating SMBH producing an Active Galactic Nuclei (AGN). As a result, AGNs are among the brightest and most energetic processes known in astronomy. As with any astronomical object, AGNs have recognizable signatures in different wavelengths. Radio-loud AGN (RLAGN) detections originate from relativistic charged particles gyrating in a magnetic field producing non-thermal synchrotron emission which is visible in radio wavelengths. Classical RLAGNs are characterized by either extended radio lobes jetting off perpendicular to the plane of the galaxy or a compact radio detection localized to the galaxy's center. Not only bright, AGNs are also fairly rare and only evident in <9 % of galaxies with 15-20% of AGNs presenting radio loud features (Kellermann et al. 1989). Researchers theorize that the SMBH becomes active only for short phases in a galaxy's life, though, their inception is unknown in its entirety (Schawinski et al. 2015). Current research suggests AGN fueling relies on the SMBH engine itself as well as the environment and collisional history of its host galaxy (Lynden-Bell 1969; Struck 1999). Fuel comes in the form of cool neutral hydrogen and its supply is essential to AGN longevity. To obtain this fuel, AGNs draw on local gas and stars or, in the case of a galactic collision, from the interaction with another galaxy. Large scale environmental factors, such as a galaxy's membership in a cluster, can impact the fueling of AGNs (Hlavacek-Larrondo et al. 2022).

Corresponding author: Mary Rickel
rickel.16@buckeyemail.osu.edu

1.2. *Galaxy Clusters*

Clusters are groups of galaxies bound by a gravitational potential well and marked by a dense, hot, and diffuse Intra-cluster Medium (ICM). Galaxies within a cluster are subjected to a greater number and variety of interactions such as galaxy-galaxy collisions and harassment compared to field galaxy counterparts. As galaxy harassment and collisions increase, the potential for an SMBH to acquire enough fuel to become active also increases.

Clusters are dynamic large scale structures which have the potential to merge with other clusters much like their individual constituent galaxies do. According to Bilton et al. (2020), AGN activity is heightened in merging clusters compared to the kinematically relaxed counterparts.

1.3. *Radio-Loud AGN in Clusters*

In a cluster, galaxies are also burdened with navigating the ICM. Acting as a drag force, the ICM can bend radio lobes to varying degrees (Miley et al. 1972; Begelman et al. 1979). In some cases, the ICM can even strip off gas from a galaxy in a process called ram pressure stripping. The presence of bent tails indicate the galaxy's membership to a cluster.

1.4. *Motivation*

As examined in Bilton et al. (2020), AGN activity is heightened in merging clusters compared to the kinematically relaxed counterparts. We examine each AGN in the Bilton et al. (2020) sample for a radio detection as not every AGN will produce a radio emission. In doing so, we aim to learn about the proportion and types of RLAGNs in merging and non-merging clusters.

In this project, we examine how large scale structure, such as a galaxy's membership to a cluster, influences AGN fueling. We do this by determining RLAGN population proportions in merging and non-merging clusters. In doing this, we aim to gain insight on the different physical mechanisms governing the RLAGN proportions and how it varies across the two dynamical states.

2. SAMPLE

In Bilton et al. (2020), the authors selected a sample of 33 galaxy clusters using the X-ray Clusters Database (BAX) and further populated each cluster with galaxies from the Sloan Digital Sky Survey Data Release 8. Each cluster was classified as merging or non-merging depending on their relative intensity member galaxy substructuring– a proxy for determining cluster kinematic status– resulting in 8 dynamically active (merging) and 25 dynamically relaxed (non-merging) clusters. Each member AGN was selected via a strict criteria of log10([N II]/Hα) $\geq$ -0.32 and EWHα $\leq$ 6Å, providing samples of 70 merging and 225 non-merging AGN sub-populations. This strict criteria aimed to remove Broad-Line AGN, LINERs, and starburst galaxies from the analysis.

We use the cluster and AGN catalogs from Bilton et al. (2020) to look for RLAGNs. We found 11 of the 33 clusters were captured by the LoTSS survey. Within this sample, we found one cluster, Abell 119, was only half covered by the Sloan Digital Sky Survey and was therefore discarded from the analysis. As a result, our subsample consisted of 10 clusters fully covered by LoTSS. The catalog contained the dynamical classification of the 10 clusters (6 non-merging and 4 merging), their central coordinates, and the coordinates of the known AGN sources (Table 1).

Table 1. Clusters Covered by LoTSS

Cluster	R.A.	Dec.	z
Abell 1066	159.84966	5.17253	0.070
Abell 1367	176.12305	19.83905	0.022
Abell 1656	194.95305	27.98069	0.023
Abell 1795	207.25218	26.58523	0.062
Abell 1991	223.62593	18.63088	0.044
Abell 2029	227.73334	5.74472	0.077
Abell 2033	227.86748	6.36213	0.082
Abell 2061	230.31378	30.65463	0.078
Abell 2065	230.67757	27.72263	0.073
Abell 2069	230.99141	29.8905	0.116
Abell 2199	247.16042	39.55167	0.030
Abell 2255	258.12936	64.09258	0.081
Abell 2670	358.5423	-10.40504	0.076
Abell 0426	49.65165	41.51506	0.018

3. DATA

To examine the radio characteristics of the AGN in a sample of radio galaxies we use data from the LOFAR Two-meter Sky Survey (LoTSS). Data Release 2 from the ongoing LOw-Frequency ARray (LOFAR) Two-metre Sky Survey (LoTSS) utilizes a bandwidth of 120-168 MHz images covering 27% of the northern sky (Shimwell et al. (2022)). The survey's resolution is $6''$with a central frequency of 144 MHz and a median RMS sensitivity of 83 μJy/beam.

4. ANALYSIS

Using each cluster's mean recessional velocity (czm), we divide by the speed of light to obtain the mean redshift of the respective cluster.

$$z = \frac{czm}{c} \tag{1}$$

To convert the $r_{\rm virial}$ in the Bilton+20 catalog from units of r_{200}, 200 times the critical density of the uni-

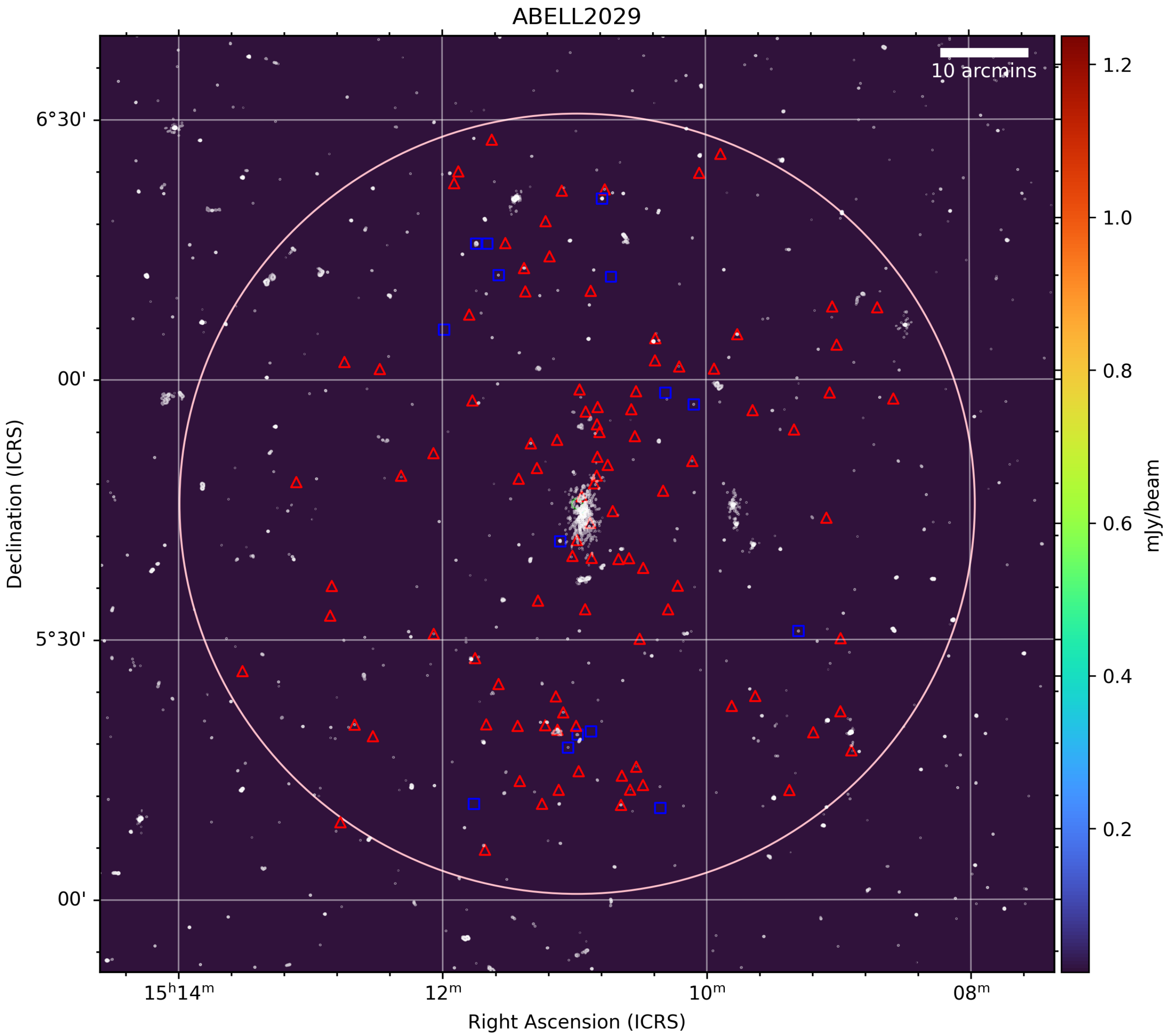

Figure 1. Galaxy Cluster Abell 2029 from LoTSS 144 MHz survey. Blue boxes correspond to the coordinates of known AGN sources in the Bilton et al. (2020) catalog. Red triangles are non-AGN sources as classified by the Bilton et al. (2020) catalog. Cluster virial radius is plotted in white. Scale bar is 10'.

verse, in to angular units, we divide by a python calculated constant ($a_{kpc-arcmin}$) which converts linear distance to angular distance from the clusters redshift (z).

$$r_{200} = \frac{r_{200}1000}{a_{kpc-arcmin}z} \tag{2}$$

We determine the size of the images required to capture the entire cluster as 2× the virial radius of the farthest AGN in units of arcminutes.

$$r_{\text{virial}} = \max(r_{\text{virial}}) * r_{200} \tag{3}$$

With the central coordinates and image size, we requested images from the Low Frequency Array (LOFAR) Two-Metre Sky Survey (LoTSS) that contained the each cluster, respectively. Figure 1 depicts an example of the large cluster image containing AGN/Non-AGN sources and cluster virial radius.

Once the images were obtained, we made $36'' \times 36''$cutouts of each known AGN source and examined for a radio detection. A radio detection is defined to be ≥ 2 contours at a 4 sigma base localized at the AGN coordinate from the Bilton et al. (2020) catalog. For each

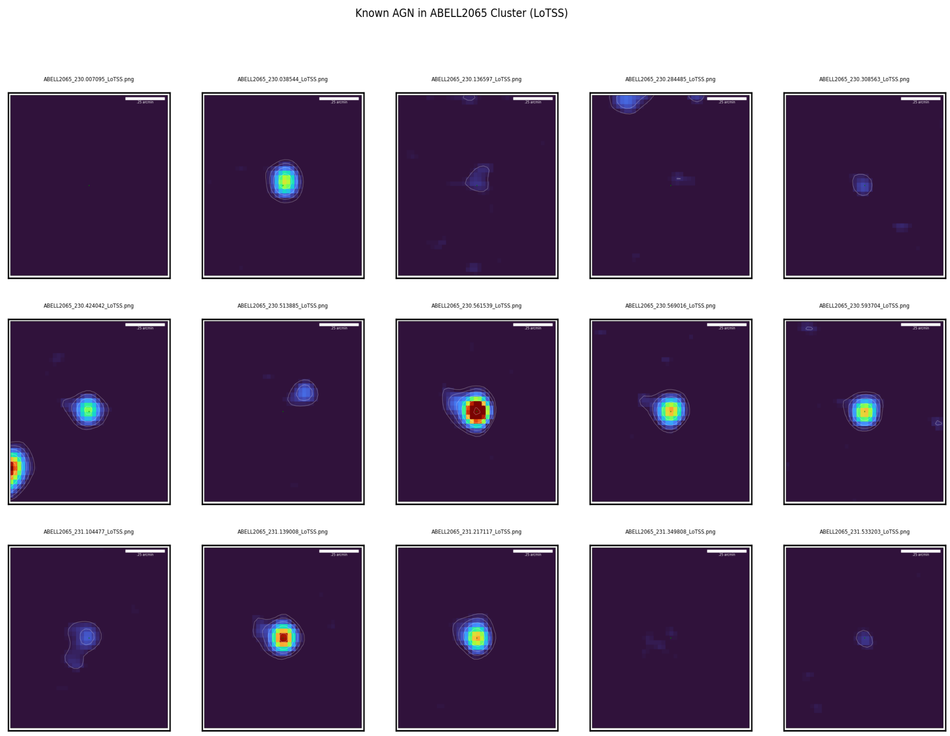

Figure 2. Radio cutout of all optically defined AGN as classified in the Bilton et al. (2020) catalog for Abell 2065. Images are from LoTSS 144 MHz survey. Scale bar is 12".

Table 2. RAGN Statistics

Cluster Name	Status	AGN	RAGN	Compact	Extended	Comp. Ext.
Abell 1367	NONmerging	3	3	0	2	1
Abell 1795	NONmerging	6	4	2	0	2
Abell 2029	NONmerging	15	13	1	8	4
Abell 2061	NONmerging	15	10	8	0	2
Abell 2065	NONmerging	15	11	3	1	7
Abell 2069	NONmerging	10	6	4	1	1
TOTALS NM:		**64**	**47**	**18**	**12**	**17**
TOTALS NM AVG:		**10.67**	**7.83**	**3.00**	**2.00**	**2.83**
Abell 2255	Merging	11	8	5	0	3
Abell 426	Merging	4	4	1	2	1
Abell 2033	Merging	7	5	1	3	1
Abell 1991	Merging	8	6	2	1	3
TOTALS M:		**30**	**23**	**9**	**6**	**8**
TOTALS M AVG:		**7.50**	**5.75**	**2.25**	**1.50**	**2.00**

Note—Columns 3-7 are the number of sources that are classified as the column header.

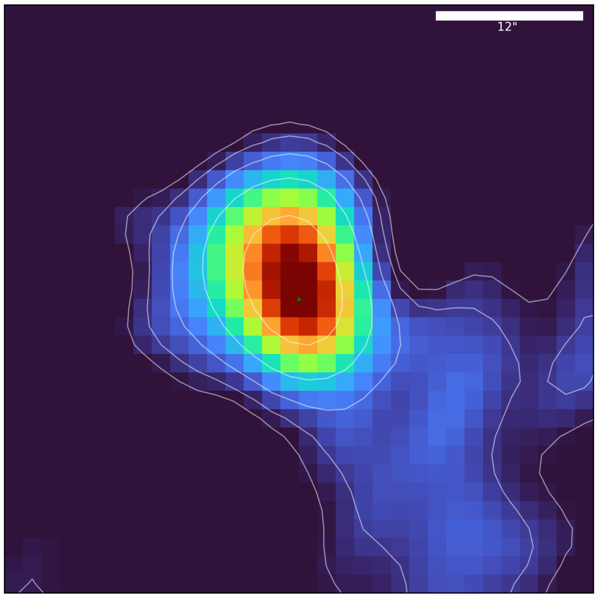

Figure 3. AGN from Abell 2033 (merging) from LoTSS 150 MHz survey. RLAGN classified as Extended. Scale bar is 12″

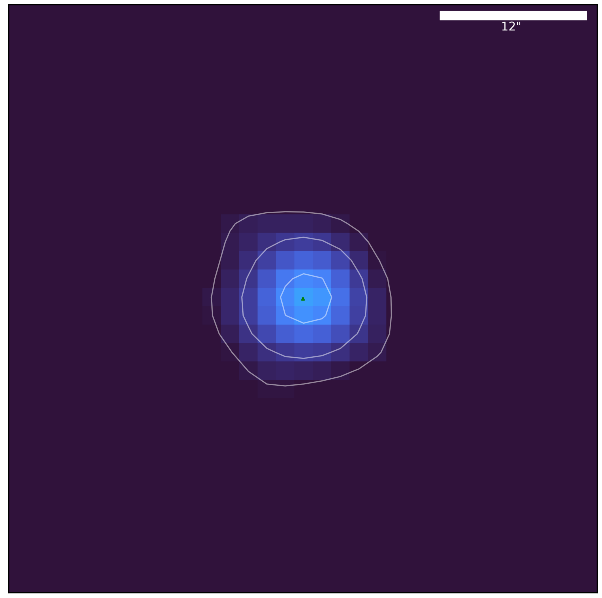

Figure 4. AGN from Abell 2061 (non-merging) from LoTSS 150 MHz survey. RLAGN classified as Compact. Scale bar is 12″

cluster, a tile was created to represent all known AGN members within the cluster (Figure 2).

If a radio detection is present, it is further classified as extended, compact extended, or compact. The detection classifications are determined by the following methodology; extended emission is > 2x the resolution of the survey (12″) Figure 3, compact extended emission is <2x the resolution of the survey but with small scale extended emissions such as an arm Figure 5, compact emission is <2x the resolution of the survey Figure 4. We utilize 2x the beam size of the survey to maintain a conservative estimate on the morphological classifications. Once classified, we normalize our populations to get a preliminary understanding of the relative proportions of detections across merging and non merging clusters.

5. RESULTS AND DISCUSSION

Though small number statistics play a role, on a first pass through radio morphology classification, on average, we see more total AGN, radio detections, extended, compact, and compact extended sources in non-merging clusters. As shown in Table 2

We will continue to make the radio classification system more robust and understand how the merging/non-merging classification affects our results.

6. SUMMARY

Utilizing a subsample of 10 clusters from Bilton et al. (2020), their optically defined AGN galaxy members,

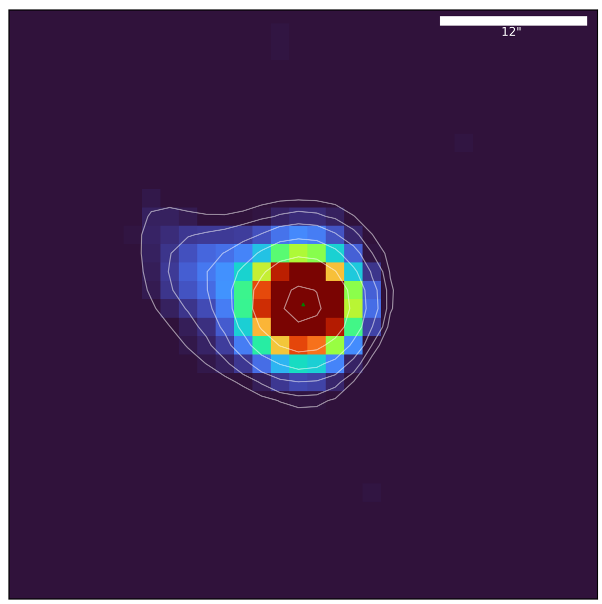

Figure 5. AGN from Abell 2065 (non-merging) from LoTSS 150 MHz survey. RLAGN classified as Compact Extended. Scale bar is 12″

and images from LoTSS, we determine on average, we see more total AGN, radio detections, compact, and compact extended sources in non-merging clusters.

7. ACKNOWLEDGMENTS

M.R. A very special thank you to Emily Moravec who provided incredible mentorship, the opportunity to work on this project, and supported every aspect of the project from data acquisition to analysis.As well, many thanks to our collaborators Lawrence Bilton and Yjan Gordon who both provided the catalogs published in Bilton et al. (2020) and provided additional support in the analysis of our results. Additional specialized coding support came from GBO staff member Victoria Catlett and GBO summer student Elizabeth Lowe. Lastly, a thank you to the entire GBO staff who supported the summer students throughout the 12 week program– especially William Armentrout and Brenne Gregory who coordinated the summer student program.

Facilities: LOFAR

Software: astropy (Astropy Collaboration et al. 2013, 2018), astropyv5.1, aplpy

REFERENCES

Astropy Collaboration, Robitaille, T. P., Tollerud, E. J., et al. 2013, A&A, 558, A33, doi: 10.1051/0004-6361/201322068

Astropy Collaboration, Price-Whelan, A. M., Sipőcz, B. M., et al. 2018, AJ, 156, 123, doi: 10.3847/1538-3881/aabc4f

Begelman, M. C., Rees, M. J., & Blandford, R. D. 1979, Nature, 279, 770, doi: 10.1038/279770a0

Bilton, L. E., Pimbblet, K. A., & Gordon, Y. A. 2020, MNRAS, 499, 3792, doi: 10.1093/mnras/staa3154

Hlavacek-Larrondo, J., Li, Y., & Churazov, E. 2022, arXiv e-prints, arXiv:2206.00098. https://arxiv.org/abs/2206.00098

Kellermann, K. I., Sramek, R., Schmidt, M., Shaffer, D. B., & Green, R. 1989, AJ, 98, 1195, doi: 10.1086/115207

Lynden-Bell, D. 1969, Nature, 223, 690, doi: 10.1038/223690a0

Miley, G. K., Perola, G. C., van der Kruit, P. C., & van der Laan, H. 1972, Nature, 237, 269, doi: 10.1038/237269a0

Noordeh, E., Canning, R. E. A., King, A., et al. 2020, MNRAS, 498, 4095, doi: 10.1093/mnras/staa2682

Schawinski, K., Koss, M., Berney, S., & Sartori, L. F. 2015, MNRAS, 451, 2517, doi: 10.1093/mnras/stv1136

Shimwell, T. W., Hardcastle, M. J., Tasse, C., et al. 2022, A&A, 659, A1, doi: 10.1051/0004-6361/202142484

Struck, C. 1999, Physics Reports, 321, 1, doi: 10.1016/s0370-1573(99)00030-7